

## Seismic Performance and Vulnerability Assessment of Existing Buildings with Infill Wall Panels

P. R. Barbude<sup>1</sup>, Dr. T. N. Boob<sup>2</sup>

<sup>1</sup>Civil Engineering (Research scholar), DMCE -Mumbai University, NaviMumbai,India;

<sup>2</sup>Civil Engineering (Principal), N P Hirani Institute of Polytechnic Pusad -, Pusad, India;

**Abstract:** The concept or the design criteria for seismic structures in Indian code is based on the maximum force developed in the members with displacements being checked at the end of the design. However, from the acceleration and displacement response spectrums it is seen that the forces do not form a correct design estimate for design of high rise structures, it is seen that the displacements and the rotations form better estimates of design criteria for high rise structures. This objective is achieved by performance based design. This report presents performance based analysis and vulnerability assessment of four existing structures assuming no strength degradation taken place. Along with this the effect of infill walls is also considered in the analysis as infills attribute a considerable lateral stiffness to the structure.

**Keywords:** Nonlinear performance based analysis, Vulnerability assessment, Effect of URM infills in seismic analysis, Fragility curves

Date of Submission: 11-04-2020

Date of Acceptance: 27-04-2020

### I. INTRODUCTION

Most of the past research on seismic response of the building was done on simple 3d portal framed structure and very few were existing buildings, along with this the effect of infill walls was also not considered as infills were considered to be non-structural elements, however it was seen that inclusion of effect of infills increased the later stiffness by a considerable amount, it also changed the performance of the building. The performance of bare framed structure and infill framed structure was compared using incremental dynamic analysis (AmirhosseinOrumiyehi et al.). (Ahmed Ghobarah) addressed life safety in case of minor earthquake, damage control in case of moderate earthquake and collapse prevention in major earthquake. Different analytical models of masonry infill for nonlinear material properties were compared by using single strut, 3 strut and finite element model by (Hemant B. Kaushik et al.). The damage occurring to the structures after a seismic event was earlier characterized qualitatively i.e. either by visual inspection or by the quantum of economic loss occurring. Soon a need for quantifying the damage was necessitated and the concept of fragility curves was derived. Fragility curves indicate relation between the intensity measures of an earthquake to the probability of failure. (Murat Serdar et al.) developed fragility curves for reinforced concrete frame buildings of 3, 5 and 7 storey in Istanbul designed according to Turkish seismic code design (1975) using incremental dynamic analysis was performed to obtain yield and collapse capacity of the building based on which the fragility curves were developed for spectral displacement, pseudo spectral acceleration, peak ground acceleration, inter storey drift and elastic spectral acceleration. The aim of this study is to evaluate the performance, response reduction factor and assess the vulnerability of four existing buildings namely Pirang tower (G+11), Venus tower (G+11), Kings tower (G+14) and Riddhi tower (G+20). To achieve this the structures were analysed in Zone III (Mumbai), Pushover analysis was carried on the structures modelled in SAP2000 v20, complying with the procedure given in Applied Technology Council (ATC) 40. Damage states were defined from the Hazus MH 2.1 manual and fragility curves are plotted in excel.

### II. BUILDING MODELS

The details of the building models considered and the architectural plans are given in this section.

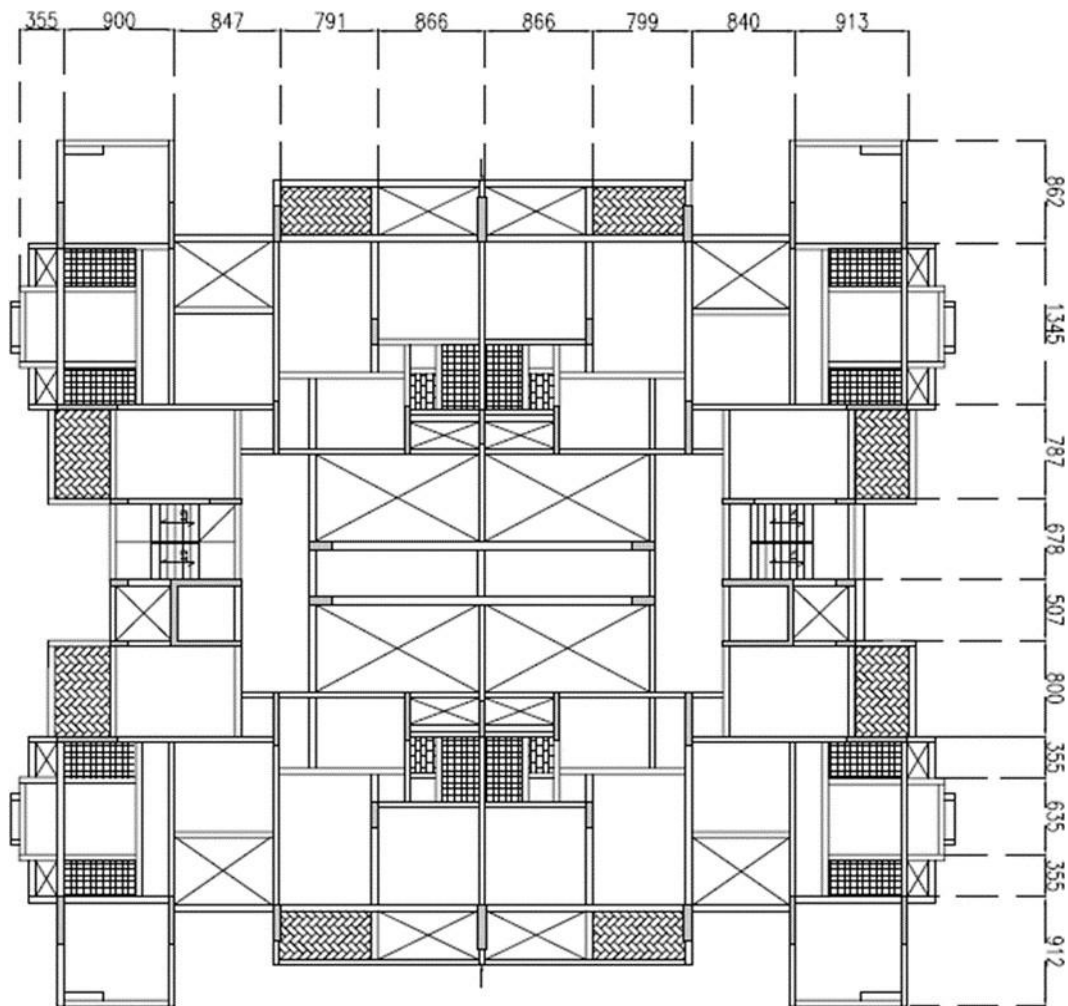
Table 1 shows the details of the buildings.

Table 1 Salient features of building

Description	Salient Features			
	Pirang Tower	Venus Tower	Kings Tower	Riddhi Tower
Floor	G+11	G+11	G+14	G+20

Floor to Floor height	2.9m	3.1m	3.1m	3.1m
Height of Structure	35.25m	38.4m	47.7m	66.3m
<b>Loading</b>				
<b>Dead Load</b>				
Floor Finish (kN/m <sup>2</sup> )	1.5	1.5	1.5	1.0
Ext. Wall (kN/m)	6.5	11.2364	10.397	7.0632
Int. Wall (kN/m)	6.074	11.2364	10.397	7.0632
Parapet (kN/m)	6	7.5	7.5	7.5
<b>Live Load</b>				
Floor Live (kN/m <sup>2</sup> )	2	2.5	2.5	2.5
Roof Live (kN/m <sup>2</sup> )	2	1.5	1.5	1.5
<b>Material</b>				
<b>Concrete</b>				
Grade in Beams	M30	M30	M30	M45
Grade in Columns	M40	M30	M30	M45
<b>Steel</b>				
Grade in Beam	Fe 415	Fe 415	Fe 415	Fe 500
Grade in Columns	Fe 415	Fe 415	Fe 415	Fe 500
<b>Seismic Data</b>				
Zone	III	III	III	III
Location	Mumbai	Mumbai	Mumbai	Mumbai
Response Red Factor	5	5	5	5
Soil Type	Hard	Hard	Hard	Hard
Damping	5%	5%	5%	5%

**III. BUILDING KEY PLANS**



**Figure 1** Pirang tower plan

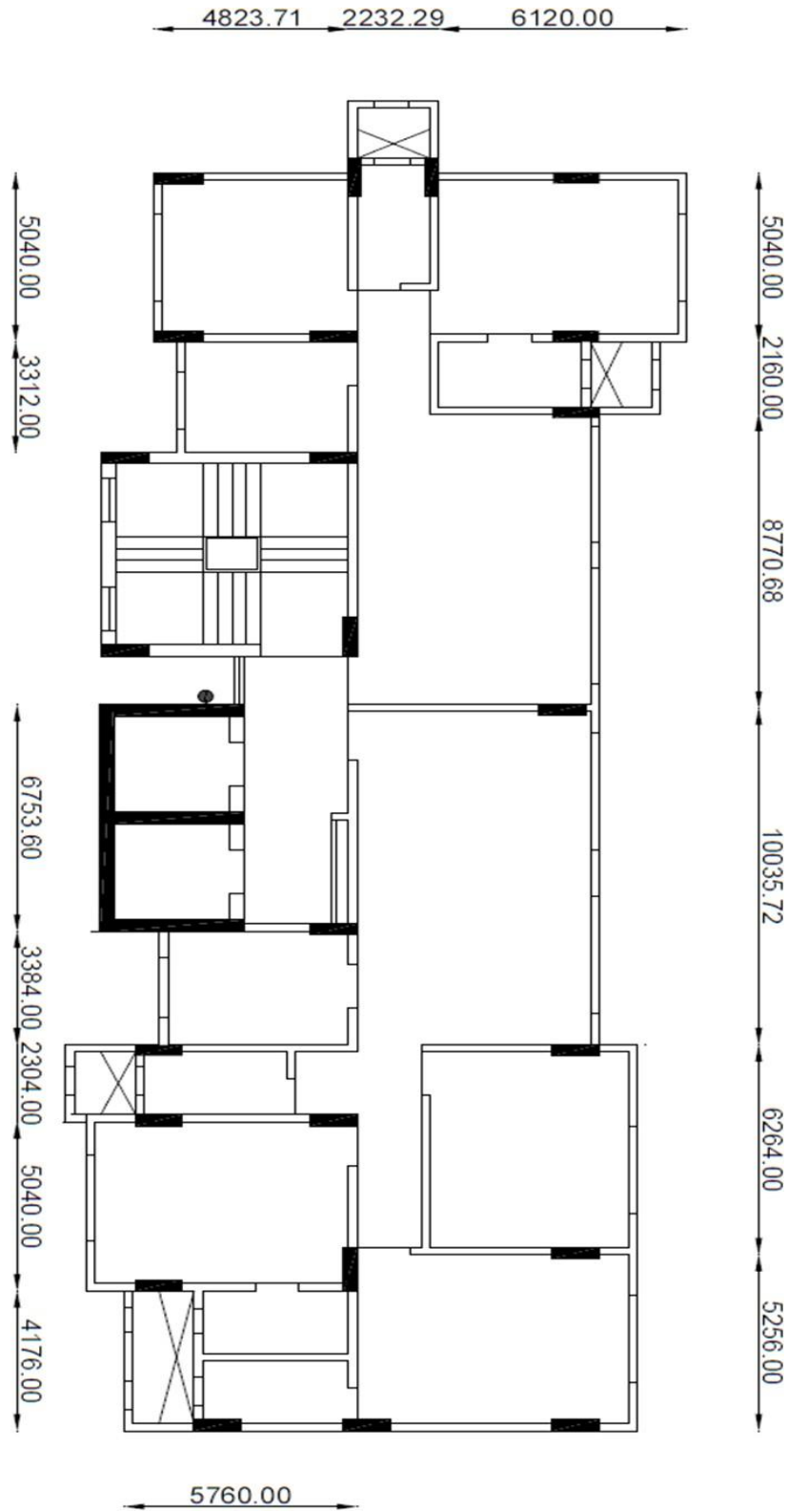


**Figure 2** Venus tower plan

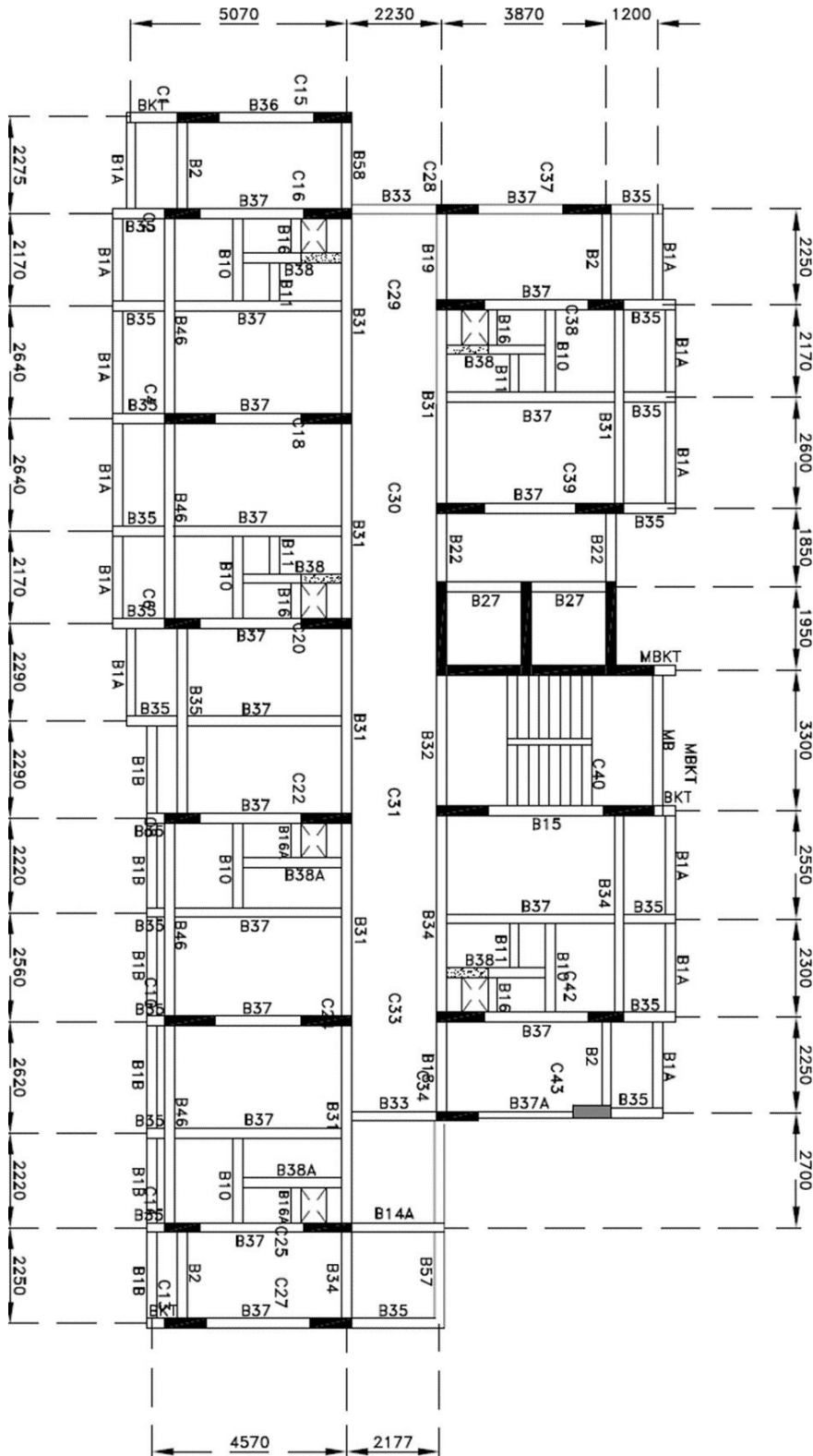


Figure 3 Kings tower plan

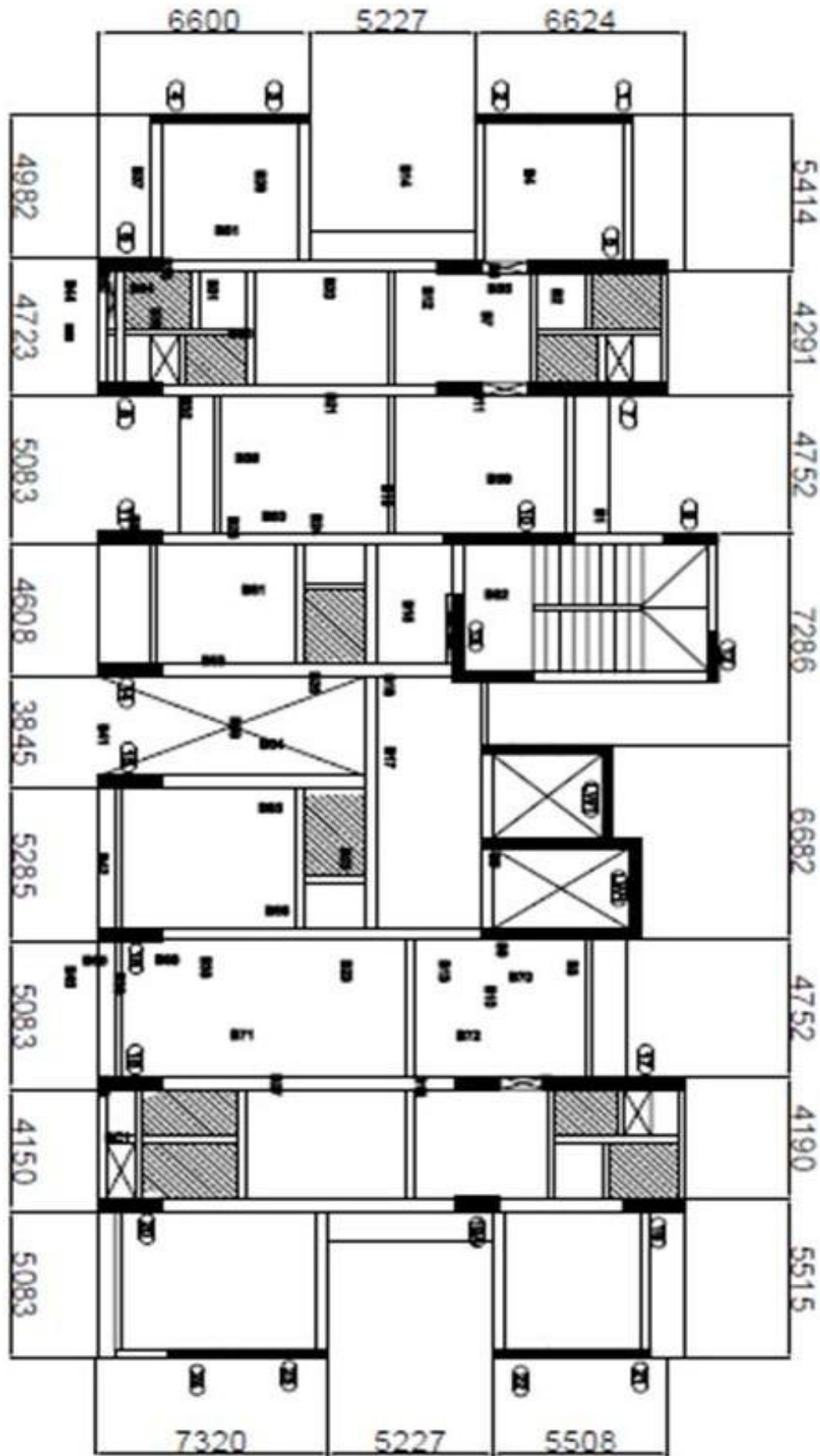


Figure 4 Riddhi tower plan

Figure 1, Error! Reference source not found.,

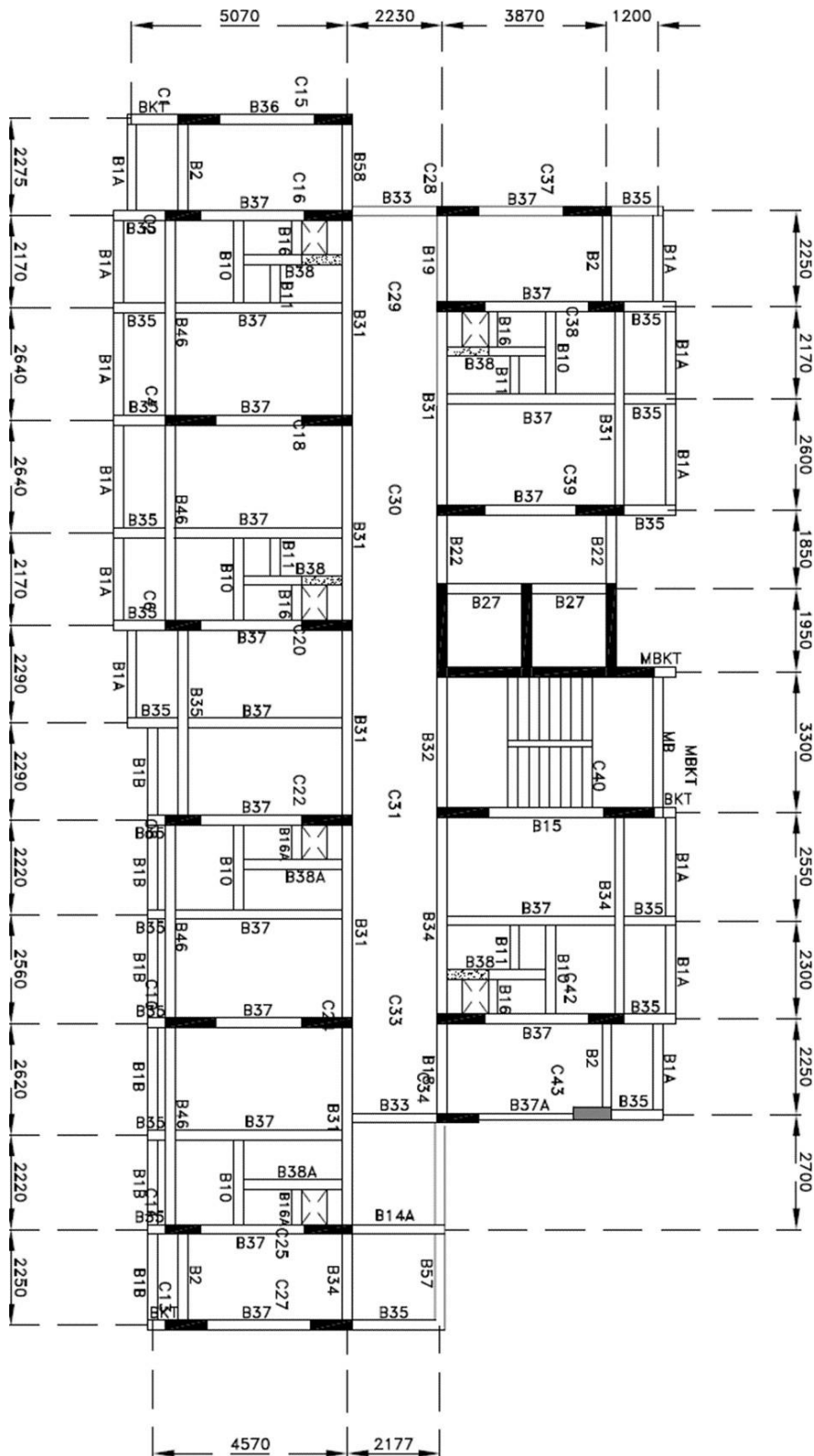


Figure 3 and Figure 4 show the auto cad model plans of Pirang tower, Venus tower, Kings tower and Riddhi tower respectively considered for analysis, all dimensions are in mm. The AutoCAD plans are architectural plans and suitable data which is not clearly states has been assumed for conversion to structural plan for using in the project.

#### IV. MODELLING OF INFILL WALLS

Infill walls are also modelled as diagonally connected frame elements in SAP 2000. In a seismic event, due to lateral forces the nature of forces vary along the length of the structure, due to this diagonal compressive and tensile forces are setup in the infills, as infills are weak under tension the tension limit in the infill is neglected and the infill is thus modelled as diagonal element carrying axial compressive force. The dimensions of the infills are such that the width is equal to the width of masonry wall and the depth is as defined in the clause 7.9.2.2 (IS 1893:2016) and is given by equation 1

$$w_{ds} = 0.175 * \alpha_h^{-0.4} * L_{ds} \tag{1}$$

Where,

$$\alpha_h = h \left( \sqrt[4]{\frac{E_m t \sin 2\theta}{4E_f I_c h}} \right) \tag{2}$$

$E_m$  and  $E_f$  are the moduli of elasticity of the materials of the URM infills and RC MRF,  $I_c$  is the moment of inertia of adjoining columns, 't' is the thickness of the infill wall,  $\theta$  is the angle of diagonal strut with the horizontal and  $L_{ds}$  is diagonal length of equivalent strut for infills.

Experimental results of C. W. Ross (1941) & H. B. Kaushik et al. (2007) were used for procuring the material properties of the infill. Table shows the material properties used.

**Table 2** Material properties of infill

Description	Value	Units	Reference
Unit weight	1920	kg/m <sup>3</sup>	H. B. Kaushik et al. (2007)
Coefficient of thermal expansion	0.000006	deg per m	C. W. Ross (1941)
Mortar Mix	1:0.5:4.5	Cement: Lime: Sand	H. B. Kaushik et al. (2007)
Compressive stress of bricks (fb)	20.8	MPa	H. B. Kaushik et al. (2007)
Compressive stress of mortar (fj)	15.2	MPa	H. B. Kaushik et al. (2007)
Prism Stress (Brick+Mortar) (fm)	6.6	MPa	H. B. Kaushik et al. (2007)
Modulus of Elasticity (Em)	3800	MPa	H. B. Kaushik et al. (2007)

#### V. NONLINEAR SEISMIC ANALYSIS

Both linear and nonlinear methods can be used to perform seismic analysis, however the response of the structure using elastic method was limited to the first yielding in the structure and subsequent force and moment redistribution is not done. It is known that the structure does not deform only till the first yielding but the response goes in to the nonlinear part as well. Inelastic methods are better at estimating response of the structure by identifying modes of failure for collapse of the structure.

Higher mode effect

The period of vibration is directly proportional to square root of the height of the structure, therefore the shorter structures have lesser time period of oscillations as compared to high rise structures. Generally, the time period of oscillation in short structures is less than 1 sec. Consider the response spectra given in IS 1893:2016 showing time periods for different modes in short structures as shown in Figure 5.

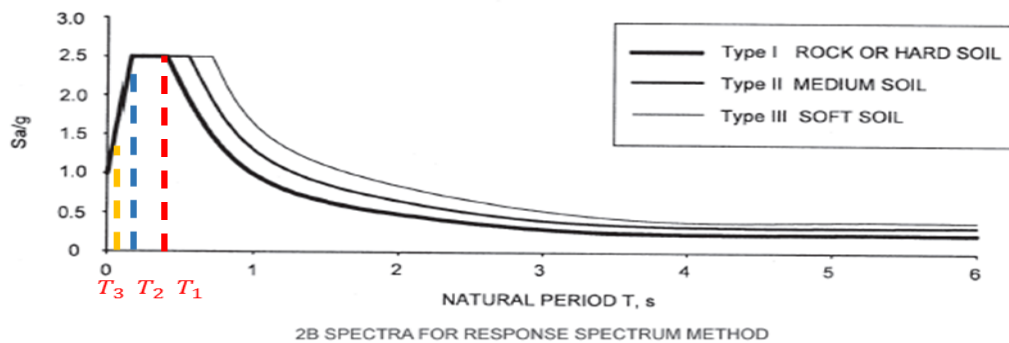


**Figure 5** Higher mode effect for short structures

The dashed red line (T1) shows the time period for fundamental mode of an arbitrary short structure. The subsequent 2<sup>nd</sup> & 3<sup>rd</sup> modes have higher frequency and therefore lower time period. The 2<sup>nd</sup> & 3<sup>rd</sup> mode time periods are shown as dashed blue line (T2) and dashed yellow line (T3) respectively. It can be observed from Figure 5 the pseudo spectral acceleration keeps on decreasing for subsequent modes and hence the force developed in the members is lesser. Therefore, the fundamental mode is the most important one in short structures. Consider the response spectra given in IS 1893:2016 showing time periods for different modes in high rise structures as shown in Figure 6.

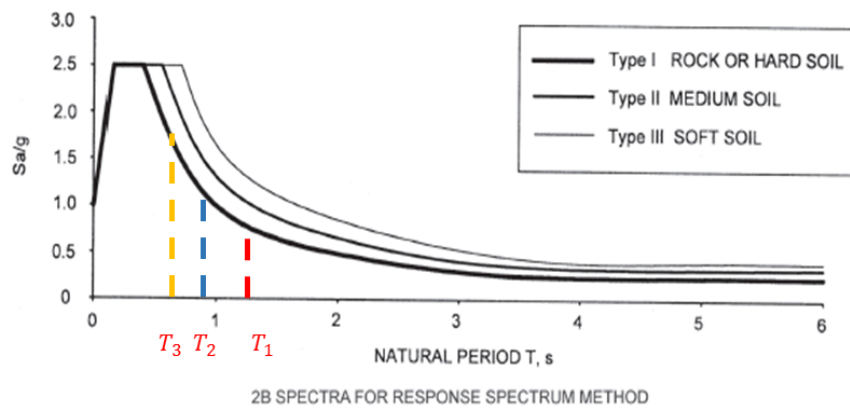


Figure 6 Higher mode effect for high rise structures

As similar to previous case T1 is the time period of fundamental mode shown in dashed red line, T2 is the time period of second mode shown in dashed blue line and T3 time period of third mode shown in dashed yellow line. As observed from Figure 6 as the subsequent modes are considered the pseudo spectral acceleration increases up to certain modes therefore the forces set up in the members are higher in the higher modes. Therefore, it is seen that for high rise structures higher mode effect has to be considered. Therefore, modal pushover analysis has been considered for all the models considering the mass participation formed in particular mode for a particular direction of seismic oscillation.

### VI. SEISMIC VULNERABILITY

The fragility curves are cumulative distribution functions of the conditional probability being in or exceeding a particular damage state, and is given by (HAZUS MH 2.1) as described in equation 3.

$$P \left[ \frac{d_s}{S_d} \right] = \Phi \left[ \frac{1}{\beta_{ds}} \ln \left( \frac{S_d}{S_d, d_s} \right) \right] \tag{3}$$





where,  $S_d$  is spectral displacement or any intensity measure;  $S_d, d_s$  are the median spectral displacement for damage state  $d_s$ ;  $\Phi$  is a normal cumulative distribution function, and  $\beta_{ds}$  is the standard deviation of the natural logarithm of the spectral displacement for damage state  $d_s$ , which is defined by equation 4.

$$\beta_{ds} = \sqrt{(CONV[\beta_C, \beta_D])^2 + (\beta_{T, ds})^2} \tag{4}$$

$\beta_C$  is the lognormal standard deviation parameter that describes the variability of capacity curve.  $\beta_D$  represent the variability in the demand spectrum.  $\beta_{T, ds}$  represent lognormal standard deviation parameter describing variability of threshold damage states. The damage states are classified qualitatively as well as quantitatively. The qualitative distinction of the damage states is as described in Table 3.



**Table 3** Qualitative classification of damage state (Hazus MH 2.1)

Damage State		Description
	Slight	Small plaster cracks at corners of doors and windows.
	Moderate	Large plaster or gypsum board cracks at corners of doors and windows.
	Extensive	Large diagonal cracks across shear wall panels
	Complete	Structure may have large permanent lateral displacement or be in imminent danger.

The median damage state spectral displacements for all the models are shown in

Table 4.

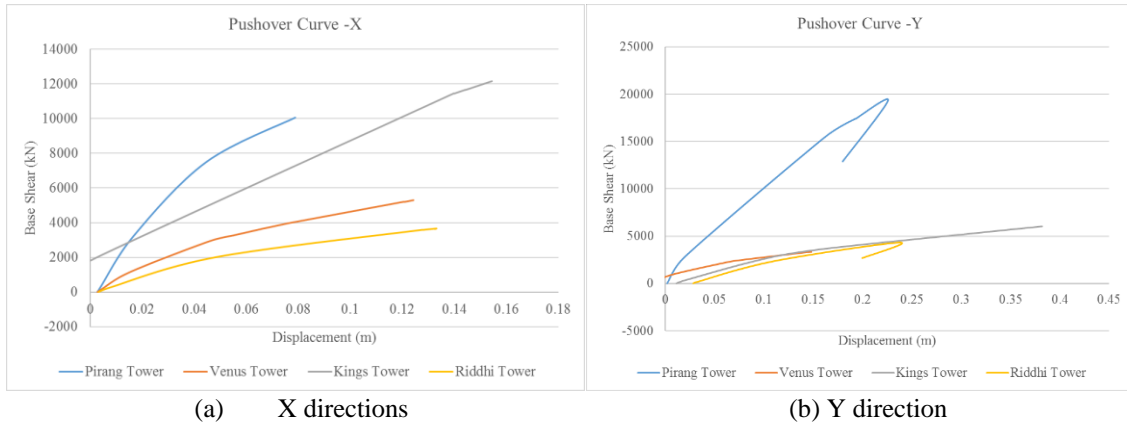
**Table 4** Damage state median values for all models.

		Damage States			
		Slight	Moderate	Extensive	Complete
Pirang	X	0.015	0.0221235	0.03013	0.054151
	Y	0.064	0.0916861	0.102066	0.1332059
Venus	X	0.018	0.0251219	0.036895	0.0722135
	Y	0.019	0.0265859	0.054797	0.1394306
Kings	X	0.025	0.0355602	0.059486	0.1312617
	Y	0.055	0.0790407	0.112213	0.2117297
Riddhi	X	0.028	0.0396015	0.059048	0.1173882
	Y	0.019	0.0272539	0.059255	0.155257

## VII. RESULTS

### Pushover analysis

This section includes results and discussions of nonlinear seismic performance analysis performed on all the towers by pushover method of nonlinear analysis which gives the behaviour of structures post elastic range. Push over curves have been plotted using modal pushover method in order to approximate the effect of higher modes. The results are depicted in graphical form only for the maximum of positive or negative condition in either directions. Push over analysis is performed as per guidelines given in (ATC40 1996) and (FEMA 356 2000). Figure 7 shows all the pushover curves obtained for each model in X & Y directions.



(a) X directions (b) Y direction  
**Figure 7** Pushover curve (a) X directions (b) Y direction

It is observed from Figure 6 1 & Figure 6 2 that as the height of the tower increases the initial stiffness of the tower decreases and the curve has lesser slope initially and then slope changes into nonlinear part. The initial stiffness in X direction are 232244 kN/m for Pirang tower (35.25m), 92416 kN/m for Venus tower (38.4m), 82346 kN/m for Kings tower (47.7m) and 63317 kN/m for Riddhi tower (66.3m). The initial stiffness in Y direction are 156390 kN/m for Pirang tower, 48548 kN/m for Venus tower, 37418 kN/m for Kings tower and 29266 kN/m for Riddhi tower.

Response reduction factor

Various components of response reduction factor are found from the SAP 2000 results and are tabulated for all the structures in

Table 5&Table 6.

**Table 5** Response reduction factor in X direction

	Pirang	Venus	Kings	Riddhi
<b>Height</b>	35.25	38.4	47.7	69.4
<b>dy</b>	28.13	27.42	28.32	29.55
<b>V<sub>v</sub></b>	6554.3225	2991.3574	2502.7713	2058.93
<b>V<sub>d</sub></b>	2450.094146	967.8084822	1291.324942	1304.461821
<b>d<sub>v</sub></b>	32.5095	41.0293	27.46	46.9736
<b>d<sub>u</sub></b>	75.897	121.391	154	132.478
<b>μ</b>	2.334609883	2.958641751	5.60815732	2.820265
<b>R<sub>μ</sub></b>	2.334609883	2.958641751	5.60815732	2.820265
<b>R<sub>s</sub></b>	2.675130877	3.090856771	1.938142151	1.578375056
<b>R<sub>r</sub></b>	1	1	1	1
<b>R</b>	6.245386984	9.144737888	10.86940609	4.451435926

**Table 6** Response reduction factor in Y direction

	Pirang	Venus	Kings	Riddhi
<b>Height</b>	35.25	38.4	47.7	69.4
<b>dy</b>	29.455	10.51	12.97	13.328
<b>V<sub>v</sub></b>	12939	1363.9379	3226.5123	1587.14
<b>V<sub>d</sub></b>	2507.13327	599.1796527	873.8942927	876.0625636
<b>d<sub>v</sub></b>	122.767	21.503	119.693	61.002
<b>d<sub>u</sub></b>	178.159	160.654	335.945	237.044
<b>μ</b>	1.451196168	7.471236572	2.806722198	3.885839809
<b>R<sub>μ</sub></b>	1.451196168	7.471236572	2.806722198	3.885839809
<b>R<sub>s</sub></b>	5.160874436	2.276342152	3.692108218	1.811674264
<b>R<sub>r</sub></b>	1	1	1	1
<b>R</b>	7.489441207	17.00709074	10.36272209	7.039875974

Performance point

The point where capacity curve intersects with the spectrum curve is called the performance point. The spectral displacement at performance point is the demand displacement of the structure for a provided ground motion, the structure will not undergo spectral displacement greater than the spectral displacement of the performance point. Table 7 gives the performance point in X & Y direction Figure 8 shows the performance point

in terms of base shear vs displacement

**Table 7** Performance point in spectral coordinates in X & Y direction respectively.

Building	X		Y		Tx	Ty	Height
	Ppt SD (m)	Ppt SA	Ppt SD (m)	Ppt SA			
Pirang	0.0440	0.0843	0.8981	1.0161	28.1300	29.4550	35.2500
Venus	0.0438	0.0839	0.8641	1.2653	27.4200	10.5100	38.4000
Kings	0.0516	0.1018	1.1825	1.6353	28.3200	12.9700	47.7000
Riddhi	0.1005	0.0376	1.8040	1.7260	29.5500	13.3280	69.4000

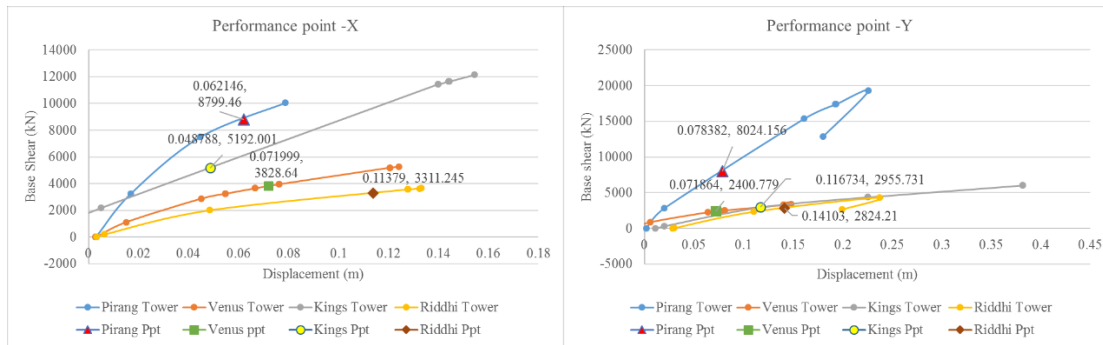


**Figure 8** Performance point in terms of displacement and base shear (a) X direction (b) Y direction

**Table 8** Performance level for all towers.

		Displacement at performance point	Drift %	Performance level
Pirang	Push X	0.062146	0.176300709	Immediate Occupancy
	Push Y	0.078382	0.222360284	Immediate Occupancy
Venus	Push X	0.071999	0.187497396	Immediate Occupancy
	Push Y	0.071864	0.187145833	Immediate Occupancy
Kings	Push X	0.048788	0.102280922	Immediate Occupancy
	Push Y	0.116734	0.244725367	Immediate Occupancy
Riddhi	Push X	0.11379	0.163962536	Immediate Occupancy
	Push Y	0.14103	0.203213256	Immediate Occupancy

As seen from

Table 8 all the buildings have drift limits less than 1% in both X & Y direction therefore the performance level for all the buildings is immediate occupancy.

**Inter storey drift**

Inter storey drifts are maximum where the storey stiffness is lowest or suddenly decreases from the above or below storey level. As it is observed from Figure 9 the ISD for Pirang tower is maximum at around 7th floor level in X & 5th floor in Y direction, for Venus tower the ISD is maximum at 9th floor in X direction and 6th floor in Y direction, for Kings tower the ISD is maximum at 3rd floor in X direction and at 12th floor in Y direction and for Riddhi tower the ISD is maximum at 10th floor in X direction and at 16th floor in Y direction.

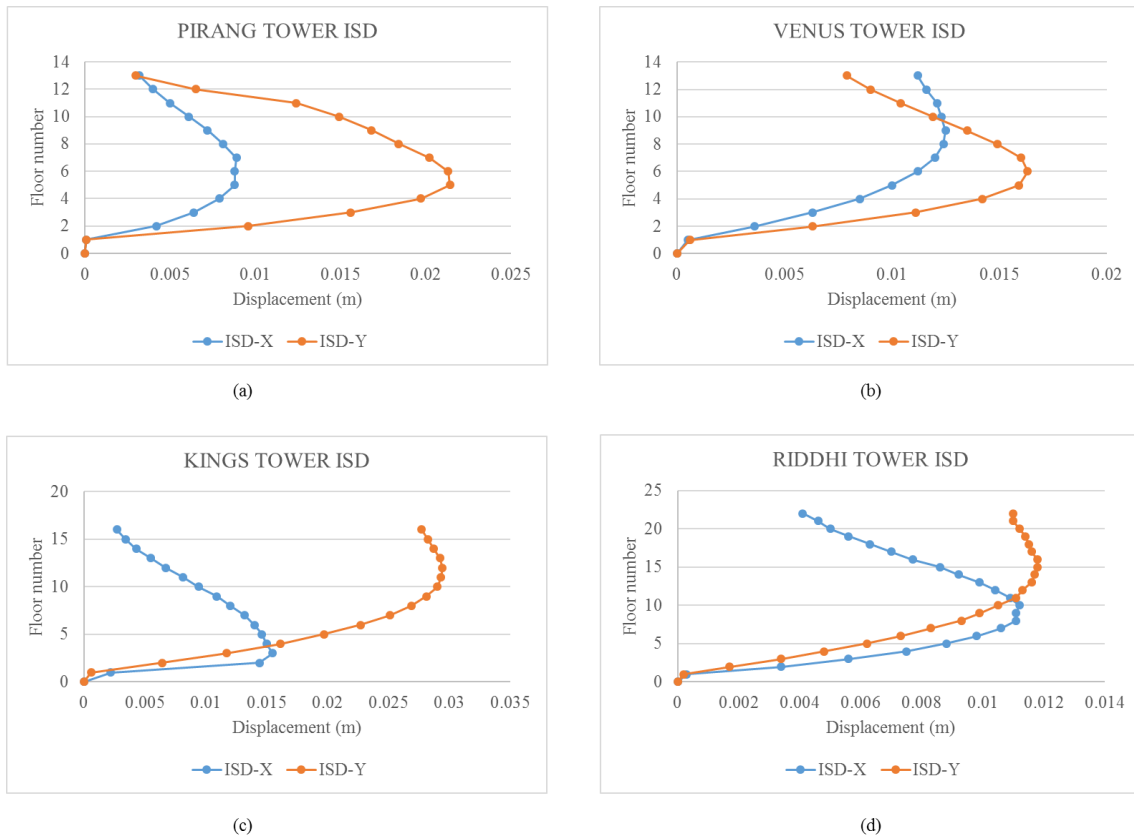


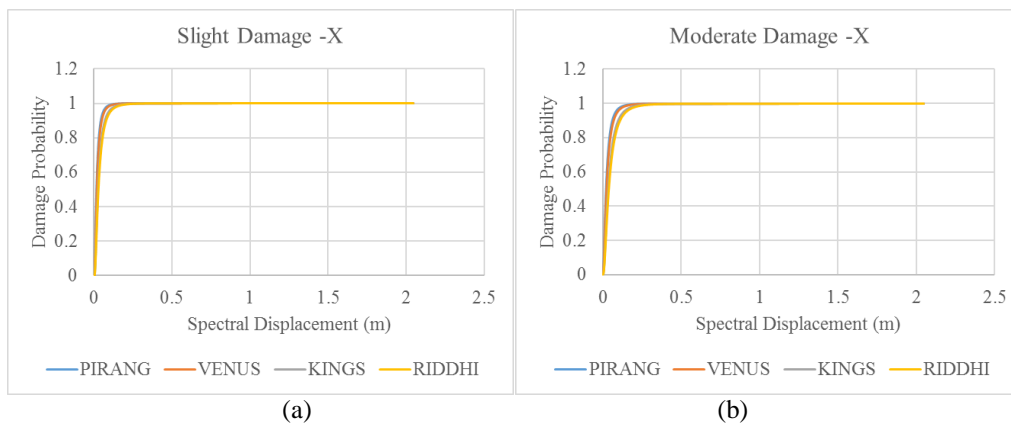
**Figure 9** (a) Pirang Tower Inter Storey drift (b) Venus Tower Inter Storey Drift (c) Kings Tower Inter Storey Drift (d) Riddhi Tower Inter Storey Drift

The storey drift limitation as per IS 1893:2016 clause 7.11.1, given as 0.004 time the height of the structure are all under specified limits

**Vulnerability Analysis**

The curves are plotted for various damage states having different median values for all the towers in X & Y direction. As per Hazus manual building type classification all concrete moment frames greater than 8 stories are classified as high rise buildings, hence lognormal standard deviation for high rise buildings having small capacity curve variability, major degradation and moderate damage variability is considered. The lognormal standard deviation of 0.8 is obtained and following fragility curves are plotted for the same.

Figure 10 shows the fragility curves for different damage states in X direction and Figure 11 shows the fragility curves for different damage states in Y direction.



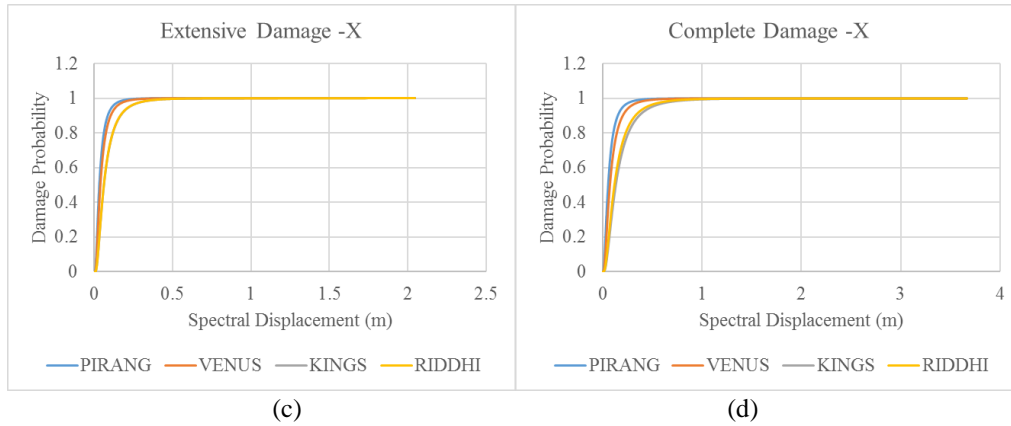


Figure 10 Fragility curves in X direction (a) Slight damage (b) Moderate damage (c) Extreme damage (d) Complete damage

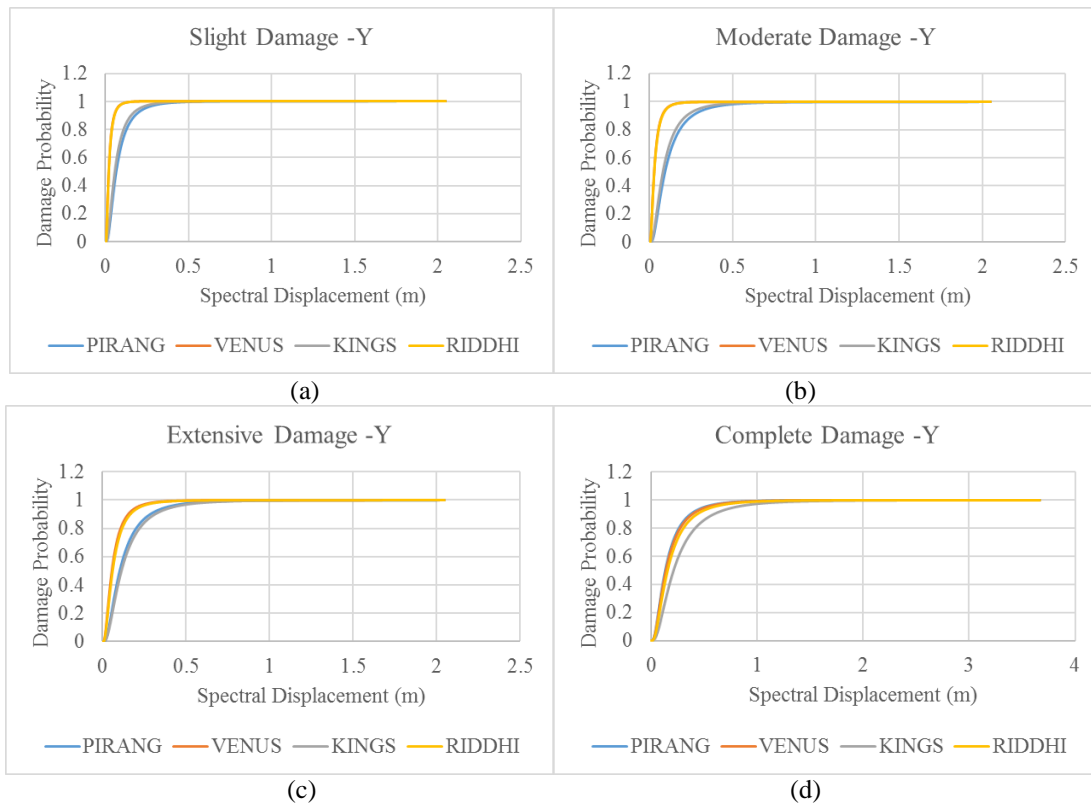


Figure 11 Fragility curves in Y direction (a) Slight damage (b) Moderate damage (c) Extreme damage (d) Complete damage

Table 9 Spectral displacement for various damage state median values in X direction

	PIRANG	VENUS	KINGS	RIDDHI
<b>Sd at Performance point</b>	0.044038	0.043803	0.051608	0.100458
<b>Sd at median of Slight Damage</b>	0.01549453	0.01759	0.024894	0.027725
<b>Sd at median of Moderate Damage</b>	0.02212599	0.025124	0.035564	0.039605
<b>Sd at median of Extensive Damage</b>	0.03013229	0.036896	0.059488	0.059049
<b>Sd at median of Complete Damage</b>	0.05415221	0.072215	0.131262	0.117389

It is observed from Table 9 that the spectral displacement values for slight and moderate damage for all the towers are below the performance point, hence these damage states can occur once the median values are exceeded. Extensive damage can occur for Pirang tower, Venus tower and for Riddhi tower but not for Venus

tower as the performance point is below the spectral displacement required for the extensive damage state to occur. Complete damage state will not occur for any of the building. The values shown in red corresponds to the damage state exceeding the value of spectral displacement at performance point.

**Table 10** Spectral displacement for various damage state median values in Y direction.

	<b>PIRANG</b>	<b>VENUS</b>	<b>KINGS</b>	<b>RIDDHI</b>
<b>Sd at Performance point</b>	0.05811	0.06728	0.07708	0.08920
<b>Sd at median of Slight Damage</b>	0.06418	0.01862	0.05533	0.01908
<b>Sd at median of Moderate Damage</b>	0.09169	0.02659	0.07904	0.02726
<b>Sd at median of Extensive Damage</b>	0.10207	0.05480	0.11221	0.05926
<b>Sd at median of Complete Damage</b>	0.13321	0.13943	0.21173	0.15526

It is observed from

Table 10 that for Pirang tower none of the damage state is exceeded as performance point is lower than the median values of all the damage states, complete damage state is not exceeded in any of the tower, except for slight damage all other damage states are not exceeded for Kings Tower. The values marked in red indicate spectral displacement greater than spectral displacement at performance point.

### VIII. CONCLUSION

1. Time period ( $T_x$  and  $T_y$ ) mentioned in Table 7 are the time period of vibration in the X and Y direction respectively for Pirang tower, Venus tower and Kings tower the vibration in X direction occurs at mode 3, thus effect of higher mode also has to be considered.
2. As observed from Table 5 & Table 6 all the response reduction factors calculated are near to or greater than 5 suggesting the codal value in IS 1893:2016 for a SMRF is on a conservative side.
3. The performance point of all the building towers suggests performance level to be immediate occupancy as seen in Table 8.
4. The inter storey drift for all the building models are within the prescribed limit.
5. From Table 9 & Table 10 Complete damage state is not exceeded for any building in X and Y direction. None of the damage state is exceeded for Pirang tower in y direction and all damage states but slight damage are not exceeded for Kings tower in Y direction.
6. The median of damage states in X direction are in increasing order as per the heights of the structures.

### REFERENCES

- [1]. ASCE 41, S. E. (2014). Seismic Evaluation and Retrofit of Existing Buildings. American Society of Civil Engineers.
- [2]. ATC19, A. T. (1995). Structural response Modification Factors. In A. t. Council. California.
- [3]. ATC40, C. S. (1996). Seismic Evaluation and Retrofit of Concrete Building. California: Applied Technology Council.
- [4]. FEMA 356, F. E. (2000). Prestandard and commentary for the seismic rehabilitation of buildings. In A. s. Engineers. Virginia: ASCE.
- [5]. HAZUS MH 2.1, B. D. (n.d.). Earthquake Loss Estimation Methodology Hazus-MH2.1. In B. D. Earthquake Committee, Earthquake Loss Estimation Methodology Hazus-MH2.1. Washington, DC.
- [6]. Hemant B. Kaushik, D. C. (2007). Uniaxial compressive stress-strain model for clay brick masonry. Journal of materials in Civil Engineering.
- [7]. IS1893:2016, B. o. (n.d.). Criteria for Earthquake Resistant Design of Structures. In IS 1893:2016 (p. 25).
- [8]. Wai-Fah Chen, E. M. (2005). Earthquake engineering for structural design. CRC Press.
- [9]. Yeudy F. Vargas, L. G. (2013). Capacity, fragility and damage in reinforced concrete buildings: a probabilistic approach. Bull earthquake eng, 2007-2033.